RESEARCH PAPER

DEVELOPMENT AND OPTIMIZATION OF LIPID NANOCONJUGATES FOR DELIVERY OF QUETIAPINE FUMARATE

Running title: Lipid Nanoconjugates for Quetiapine Fumarate Delivery

Ms Chitrali R. Talele [1], Dr. Payal N. Vaja[2], Dr. Hardik L. Varu[3], Dr. Chetan H. Borkhataria[4]

[1]Research Scholar, School of Pharmacy, Dr. Subhash University, Junagadh (362001), Gujarat, India

[2]Associate Professor, School of Pharmacy, Dr. Subhash University, Junagadh (362001), Gujarat, India

[3]Assistant Professor, School of Science, Dr. Subhash University, Junagadh (362001), Gujarat, India

[4]Assistant Professor, Department of Pharmaceutics, BK Mody Government Pharmacy College, Rajkot (360003), Gujarat, India.

Correspondence to:

Dr. Payal N. Vaja

Associate Professor, School of Pharmacy, Dr. Subhash University, Junagadh (362001), Gujarat, India.

(M) 8780541846, Email Id: payalvaja55@gmail.com

ABSTRACT

Objective: The present study aimed to develop and optimize quetiapine fumarate-loaded lipid nanoconjugates (QF-LNCs) to enhance drug encapsulation and achieve sustained drug release using a statistically guided experimental design approach.

Methods: QF-LNCs were prepared by the solvent evaporation technique using stearic acid as the lipid matrix and polyvinyl alcohol as the stabilizer. A Plackett-Burman design was employed to identify the critical formulation and process variables affecting percentage yield and encapsulation efficiency. The significant variables were subsequently optimized using a Box–Behnken design. The optimized formulation was characterized for particle size, polydispersity index, zeta potential, encapsulation efficiency, drug loading, surface morphology, Fourier-transform infrared spectroscopy, differential scanning calorimetry, X-ray diffraction, in vitro drug release, and stability according to ICH guidelines.

Results: The Plackett-Burman design identified lipid concentration, PVA concentration, and stirring speed as the most influential variables affecting formulation performance. The optimized QF-LNCs exhibited a particle size of 400.5 nm, a PDI of 0.5416, a zeta potential of −21.88 mV, and an encapsulation efficiency of 63.55 ± 1.71%, with a drug loading of 4.0 ± 0.28% (w/w). SEM analysis revealed predominantly spherical particles with smooth surfaces, while FTIR confirmed drug–lipid compatibility without evidence of chemical interaction. DSC and XRD analyses demonstrated reduced crystallinity and successful incorporation of quetiapine fumarate within the lipid matrix. The optimized formulation exhibited a biphasic release pattern with an initial burst release followed by sustained drug release, achieving 85.78 ± 2.49% cumulative release over 24 h. Drug release followed predominantly first-order kinetics ($R^2 = 0.983$) with diffusion-controlled release as indicated by the Higuchi model ($R^2 = 0.956$). Stability studies demonstrated minimal changes in physicochemical properties under refrigerated and long-term storage conditions over six months.

Conclusion: The developed lipid nanoconjugate formulation demonstrated satisfactory physicochemical characteristics, sustained drug release, and good storage stability. The statistically optimized QF-LNCs represent a promising oral drug delivery system for quetiapine fumarate with the potential to improve therapeutic performance and patient compliance. Further in vivo investigations are warranted to establish their pharmacokinetic behavior and clinical applicability.

Keywords: Box-Behnken design, Encapsulation efficiency, Lipid nanoconjugates, Plackett-Burman design, Quetiapine fumarate, Solvent evaporation, Sustained drug release

How to cite this article: Chitrali R. Talele 1 Dr. Payal N. Vaja2 Dr. Hardik L. Varu3 Dr. Chetan H. Borkhataria4. DEVELOPMENT AND OPTIMIZATION OF LIPID NANOCONJUGATES FOR DELIVERY OF QUETIAPINE FUMARATE. Int J Drug Deliv Technol. 2026;16(90s):1838-1853. DOI: 10.25258/ijddt.16.90s.186.

1. INTRODUCTION

Quetiapine fumarate (QF) is a second-generation atypical antipsychotic widely prescribed for the management of schizophrenia, bipolar disorder, and major depressive disorder. Despite its therapeutic efficacy and favorable tolerability profile, its clinical performance is limited by poor aqueous solubility, extensive first-pass metabolism, and low oral bioavailability (~9%). The drug exhibits pH-dependent solubility, being more soluble in acidic gastric fluid and poorly soluble in alkaline intestinal pH. Consequently, after oral administration, only a small fraction of the dose is absorbed in the stomach and proximal small intestine, which constitutes the primary absorption window for quetiapine fumarate. Conventional oral formulations often require frequent dosing to maintain therapeutic plasma concentrations, which may lead to fluctuations in drug levels, noncompliance, and potential adverse effects(Riedel et al., 2007).

In recent years, lipid-based nanocarriers have emerged as a promising platform for improving the solubility, stability, and bioavailability of lipophilic and poorly water-soluble drugs. Among these systems, lipid nanoconjugates (LNCs) offer distinct advantages due to their hybrid composition of a solid lipid matrix combined with surfactant stabilization, enabling both sustained release and enhanced absorption through the gastrointestinal mucosa. LNCs not only improve drug solubilization and permeability but also promote lymphatic uptake, thereby partially bypassing hepatic first-pass metabolism. Furthermore, their physiological compatibility and ability to incorporate lipophilic drugs make them an ideal alternative to polymeric nanoparticles, particularly for drugs like quetiapine fumarate that require controlled gastric release followed by sustained systemic absorption(Chauhan, 2026).

Stearic acid, a biocompatible and biodegradable long-chain fatty acid, has been widely utilized as a solid lipid for the fabrication of lipid-based nanoparticles and conjugates. It provides excellent physicochemical stability, a hydrophobic matrix for high drug loading, and controlled release characteristics. In addition, its GRAS (Generally Recognized as Safe) status and low toxicity make it suitable for oral administration(Duong, Nguyen, & Maeng, 2020). Formulating quetiapine fumarate with stearic acid through the solvent evaporation technique enables efficient entrapment of the drug within the lipid matrix, leading to improved protection from degradation and extended-release kinetics. The presence of surfactant stabilizers such as polyvinyl alcohol further enhances dispersion stability and uniform particle formation.

The present investigation aims to develop and optimize quetiapine fumarate-loaded lipid nanoconjugates (QF-LNCs) using the solvent evaporation method. Initially, a Plackett-Burman Design (PBD) was employed to screen the critical formulation and process variables affecting particle characteristics. The most significant parameters were then subjected to systematic optimization using a Box-Behnken Design (BBD) to establish their quantitative relationship with key responses, including percentage yield, particle size, and entrapment efficiency. The prepared lipid nanoconjugates were characterized for their physicochemical properties, surface morphology, drug loading, and in vitro release profile to elucidate the formulation's potential for enhanced oral bioavailability and prolonged therapeutic effect of Quetiapine fumarate.

2. Materials and Methods

2.1 Materials

Quetiapine fumarate was procured from Sigma-Aldrich Pvt. Ltd. (India). Stearic acid and polyvinyl alcohol (PVA) were purchased from Loba Chemie Pvt. Ltd., Mumbai, India. Dichloromethane and methanol (AR grade) were procured from Loba Chemie Pvt. Ltd., Mumbai, India and were used as organic solvent. Dialysis membranes (molecular weight cut-off 12 kDa) were obtained from HiMedia Pvt. Ltd., Mumbai, India. Simulated gastric fluid (SGF, pH 1.2), and simulated intestinal fluid (SIF, pH 6.8) were prepared according to United States Pharmacopeia guidelines. All other reagents and chemicals used in the study were of analytical grade and used as received without any modification. Double-distilled water was used throughout the experimental procedures.

2.2 Methods

2.2.1 Preparation of Quetiapine Fumarate-Loaded Lipid Nanoconjugates (QF-LNCs)

QF-LNCs were prepared by the solvent evaporation technique with slight modifications(Pooja, Tunki, Kulhari, Reddy, & Sistla, 2016). Briefly, 20 mg of quetiapine fumarate and stearic acid were dissolved in a dichloromethane and methanol solvent system with the aid of a magnetic stirrer to obtain a clear organic phase. Separately, an aqueous phase was prepared by dissolving PVA in distilled water under continuous stirring until a transparent solution was achieved. The organic phase was introduced into the aqueous PVA solution under magnetic stirring using an infusion pump equipped with a syringe. The flow rate of addition was varied according to the experimental design.

The resultant emulsion was further stirred at 2000 rpm for 2 hours at room temperature to allow complete evaporation of the organic solvent and solidification of the lipid matrix. The obtained nanosuspension was centrifuged at 15,000 rpm for 15 minutes under cooling conditions to recover the LNCs. The pellet was collected, dried, and rinsed three times with distilled water to remove any remaining stabilizer or unbound drug. The resulting lipid nanoconjugates were purified, followed by air-drying at room temperature until constant weight was achieved, to obtain the QF-LNCs for further

physicochemical characterization and in vitro evaluation.

2.2.2 Experimental Design for Screening of Formulation Parameters

A Plackett-Burman Design (PBD) was employed to screen and identify the most significant formulation and process variables influencing the characteristics of Quetiapine fumarate-loaded lipid nanoconjugates (QF-LNCs). The design was constructed and analyzed using Design-Expert software (Version 13, Stat-Ease Inc., Minneapolis, USA). In this study, eleven independent variables were initially selected based on preliminary trials and literature reports: Concentration of lipid (X_1), Concentration of PVA (X_2), Volume of methanol in organic phase (X_3), Stirring Speed (X_4), Stirring Time (X_5), Volume of External Phase (X_6), Surface area (X_7), Infusion Pump Flow Rate (X_8), Needle Diameter (X_9), Distance of Drop (X_{10}), and Volume of dichloromethane in organic phase (X_{11}). During formulation development, both formulation variables and process parameters were systematically varied according to the Plackett-Burman experimental design(Aboti, Shah, Patel, & Dalwadi, 2014).

Process parameters including infusion pump flow rate, needle diameter, drop distance between the needle tip and aqueous phase, and receiving vessel surface area were systematically varied according to the experimental design. These parameters were investigated because they influence droplet formation, solvent diffusion, emulsification efficiency, lipid solidification behavior, mixing dynamics, and lipid nanoconjugate formation.

Each factor was evaluated at two levels, high (+1) and low (-1), while all other experimental conditions were kept constant. The factors and their corresponding actual values are presented in Table 1. The Plackett-Burman design generated 12 screening runs for evaluation of 11 independent variables. In addition, three replicated center-point runs were included to assess experimental variability and reproducibility, resulting in a total of 15 experimental runs. % yield (Y_1) and entrapment efficiency (Y_2) were chosen as the dependent responses. The experimental data were analyzed statistically using analysis of variance (ANOVA) to determine the significance of each factor at a 95% confidence interval ($p < 0.05$). For further systematic optimization, the significant variables identified from the Plackett-Burman design were subjected to Box-Behnken design analysis.

2.2.2 Optimization by Box-Behnken Design (BBD)

In order to optimize the formulation parameters of QF-LNCs, different combinations and ratios of ingredients were explored to evaluate their influence on the response variables, namely percentage yield (Y_1), entrapment efficiency (Y_2) and particle size (Y_3). Based on preliminary screening results, three independent formulation and process variables that is lipid concentration (X_1), PVA concentration (X_2), and stirring speed (X_4) were identified as critical factors affecting the performance of the nanoconjugates. Therefore, a BBD was employed for systematic optimization and response surface analysis. The total of 15 experimental runs was generated and QF-LNCs were prepared by varying the factor levels according to the experimental design matrix, and each batch was evaluated for the respective responses(Noorulla et al., 2022).

Statistical Analysis

A second-order polynomial equation was used for mathematical modeling to establish the relationship between the independent variables (X_1, X_2, and X_4) and the dependent responses (Y_1, Y_2, and Y_3). The generalized quadratic model is represented as:

$$Y = \beta_0 + \beta_1 X_1 + \beta_2 X_2 + \beta_3 X_4 + \beta_{12} X_1 X_2 + \beta_{13} X_1 X_4 + \beta_{23} X_2 X_4 + \beta_{11} X_1^2 + \beta_{22} X_2^2 + \beta_{33} X_4^2$$

Where Y represents the dependent response (Y_1, Y_2, or Y_3), β_0 is the intercept, β_1-β_3 are linear coefficients, β_{12}-β_{23} are interaction coefficients, and β_{11}-β_{33} are quadratic coefficients. Design-Expert software (version 10.0.1.0) was used to estimate the regression coefficients along with the generation of both full and reduced models. The statistical significance of the model and separate terms was tested with Analysis of Variance (ANOVA). Three-dimensional (3D) response surface plots and two-dimensional (2D) contour plots were built to visualize the effect of independent variables and their interactions on the responses, especially to understand how formulation parameters affect yield, entrapment efficiency and particle size.

Statistical Design Validation

The following formulations were prepared and tested for the following parameters: % yield (Y_1), entrapment efficiency (Y_2), and particle size (Y_3). The experimental results were compared with the prediction results obtained using the model and the percentage prediction error was calculated. The closeness of the predicted and observed values with a small error (<5%) ensured the reliability, validity, and robustness of the developed models.

Optimization Using Desirability Function Approach

The formulation was optimized with the desirability function approach provided by the Design-Expert software. The objective was optimized multiple responses including the percentage yield (Y_1), entrapment efficiency (Y_2) and particle size (Y_3) of the nanoconjugates to achieve stable and efficient nanoconjugates. The individual desirability functions were determined for each response and overall desirability (D) was found as the geometric mean of individual desirabilities. A desirability value closer to 1 indicates a more optimal formulation. The software has produced an optimized formulation variable set that gave the best compromise of all the responses. The optimized formulation was fabricated experimentally and

analyzed for its yield, entrapment efficiency and particle size for the confirmation of the optimized results, thus establishing the effectiveness of the optimization approach.

2.2.3. Particle size, Zeta potential, and Polydispersity index (PDI)

Mean particle size, zeta potential, and polydispersity index (PDI) of the prepared QF-LNCs were determined by dynamic light scattering (DLS) using a Zetasizer Nano ZS (Malvern Instruments, UK). A freshly prepared dispersion of nanoconjugates in distilled water was analyzed at 25 °C under an applied electric field of 150 mV. Each sample was measured in triplicate (n = 3), and the results were expressed as mean ± standard deviation (S.D.)(Zielińska, Ferreira, Feliczak-Guzik, Nowak, & Souto, 2020).

2.2.4. Encapsulation efficiency (EE) and drug loading (DL)

The encapsulation efficiency and drug loading of drug in the nanoconjugates were determined by quantifying the amount of drug entrapped within the LNCs(Ding et al., 2018). Briefly, 2 mg of the dried QF-LNCs was dispersed in 10 mL of methanol and sonicated for 5 minutes to ensure complete extraction of the drug from the lipid matrix. The resulting solution was centrifuged at 15,000 rpm for 5 minutes (Remi Instruments, Mumbai, India), and the clear supernatant was analyzed for Quetiapine fumarate content using a validated UV-visible spectrophotometric method at λ_{max} 209 nm. All measurements were performed in triplicate (n = 3), and the results were expressed as mean ± S.D. The encapsulation efficiency (EE) and drug loading (DL) were calculated using the following equations:

$$\%EE = \frac{\square\square\square\square\square\square\ \square\square\ \square\square\square\square\square\square\square\square\ \square\square\square\square\ \square\square\square\square\square\square\square\square\

wavelength of 209 nm (Shimadzu 1800, Japan). The cumulative percentage drug release was calculated, and the release data were fitted into various kinetic models including zero-order, first-order, Higuchi, and Korsmeyer–Peppas equations to elucidate the mechanism of drug release from the lipid nanoconjugates. All experiments were performed in triplicate, and the results were expressed as mean ± standard deviation (S.D.).

2.2.10 Stability Studies

Stability studies were conducted to evaluate the influence of formulation additives on drug stability and to assess the physical stability of the prepared formulation under different storage temperature and relative humidity conditions. The optimized QF-LNCs formulation was tested for stability as per the International Councilfor Harmonisation guidelines and all experiments were repeated three times. The stability testing was conducted under the following three conditions: 4±2 °C (refrigerator), 25±2 °C/60±5% RH and 40±2 °C/75±5% RH (stability chamber, Hicon Instruments, N. Delhi). Samples were taken at times of 0, 1, 3 and 6 months, and the influence of storage conditions on the particle size, PDI, zeta potential and entrapment efficiency was investigated.

3. RESULTS AND DISCUSSION

3.1 Optimization of Preparation of QF-LNCs

The screening and preliminary optimization of quetiapine fumarate-loaded lipid nanocarriers (QF-LNCs) were carried out using a Plackett–Burman Design (PBD) to identify the most influential formulation and process variables affecting percentage yield (Y_1) and entrapment efficiency (Y_2). A 12-run Plackett–Burman screening design was employed for the evaluation of eleven independent variables. Three additional replicated center-point runs were incorporated to estimate experimental error and assess reproducibility, resulting in a total of 15 experimental runs. A total of fifteen experimental runs were performed by varying eleven independent variables at two levels (−1 and +1), and the obtained results are presented in Table 2.

The responses exhibited considerable variation across the experimental runs, with percentage yield ranging from 49.06% to 77.81% and entrapment efficiency ranging from 35.80% to 75.43%, indicating that the preparation of QF-LNCs was highly sensitive to changes in formulation and process variables. The Plackett–Burman design demonstrated that both formulation composition and processing conditions influenced the performance of the lipid nanocarrier system. Among the variables investigated, lipid concentration exhibited the most significant positive effect on both percentage yield and entrapment efficiency. Increasing the lipid concentration resulted in improved drug encapsulation and higher nanoparticle recovery. This may be attributed to the availability of a larger lipid matrix for incorporation of quetiapine fumarate, which minimizes drug diffusion into the external aqueous phase during emulsification and solvent evaporation. In addition, the increased lipid content enhanced the structural integrity of the lipid nanocarriers, leading to higher process yield and improved drug retention.

PVA concentration also showed a significant positive contribution to both responses. Increasing the concentration of PVA improved stabilization of the emulsion droplets and reduced droplet coalescence during nanoparticle formation. Enhanced emulsion stability facilitated efficient formation of lipid nanocarriers, resulting in improved percentage yield and higher entrapment efficiency. Formulations prepared with higher PVA concentrations generally exhibited superior drug encapsulation owing to improved stabilization of the dispersed phase during solvent evaporation.

Stirring speed was identified as another important variable influencing the formulation performance. An increase in stirring speed improved the dispersion of the organic phase within the aqueous phase, resulting in the formation of finer emulsion droplets and more uniform nanoparticles. Improved dispersion increased the interfacial surface area available for solvent diffusion and lipid solidification, thereby enhancing nanoparticle formation and drug entrapment. Consequently, higher stirring speeds were associated with increased percentage yield and entrapment efficiency within the investigated experimental range.

In contrast, other variables such as dichloromethane volume, methanol volume, stirring time, external phase volume, surface area, infusion pump flow rate, needle diameter, and drop distance exhibited comparatively smaller effects on the responses within the investigated range, indicating that these variables were less critical in controlling the preparation of QF-LNCs.

The statistical significance and reliability of the Plackett-Burman design were evaluated using normal probability plots and Pareto charts (Figure 1). The normal probability plots indicated an approximately normal distribution of the experimental data, demonstrating good agreement between the observed and predicted responses. The Pareto charts illustrated the relative contribution of each variable, with factors crossing the significance threshold identified as influential variables. The main effect plots (Figure 2) demonstrated the effect of each independent variable on percentage yield and entrapment efficiency. The direction of the lines indicated whether the effect was positive or negative, whereas the steepness of the slope reflected the magnitude of the effect. Lipid concentration and PVA concentration exhibited the steepest slopes, confirming their dominant influence on both responses.

The Plackett-Burman design efficiently identified the critical variables influencing formulation performance while requiring fewer experimental runs than conventional one-factor-at-a-time experimentation. Based on these findings, lipid concentration, PVA concentration, and stirring speed were selected for further optimization using response surface methodology.

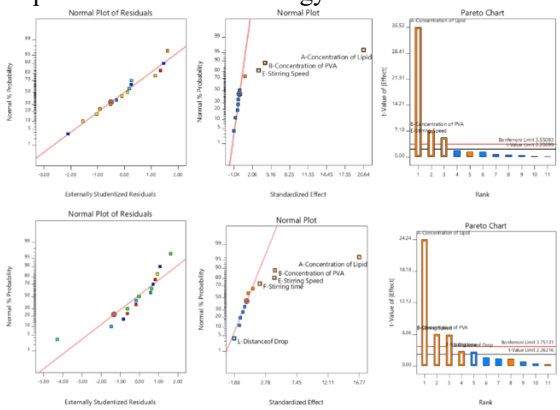

Figure 1. Normal probability plots and Pareto charts illustrating the standardized effects of formulation and process variables on (A) percentage yield and (B) encapsulation efficiency of QF-LNCs obtained using the Plackett-Burman design. Variables exceeding the significance limit were considered statistically influential.

Table 1 Independent Variables and Levels Used in Plackett–Burman Design

Factor	Variable (Unit)	Low (-1)	Center (0)	High (+1)
X_1	Lipid Concentration (mg)	300	500	700
X_2	PVA Concentration (% w/v)	0.50	0.75	1.00
X_3	Dichloromethane Volume (mL)	1	3	5
X_4	Methanol Volume (mL)	1	3	5
X_5	Stirring Speed (rpm)	1000	2000	3000
X_6	Stirring Time (h)	1	2	3
X_7	External Phase Volume (mL)	100	200	300
X_8	Surface Area (cm^2)	84.78	142.40	200.01
X_9	Infusion Pump Flow Rate (mL/h)	50	125	200
X_{10}	Needle Diameter (Gauge)	22	24	26
X_{11}	Drop Distance (cm)	10	15	20

[1]

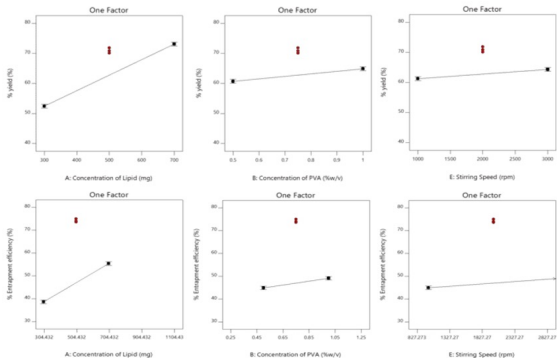

Figure 2: Main effect plots showing the influence of independent formulation and process variables on (A) percentage yield and (B) encapsulation efficiency of quetiapine fumarate-loaded lipid nanoconjugates (QF-LNCs). Steeper slopes indicate a greater effect of the corresponding variable on the response.

Table 2 Runs on Plackett Burman Design

A: Lipid Conc (mg)	B: PVA Conc (%w/v)	C: DCM Vol (ml)	D: Methanol Vol (ml)	E: Stirring Speed (rpm)	F: Stirring time (hr)	G: External phase Vol (ml)	H: Surface area (cm^2)	J: Infusion pump flowrate (ml/hr)	K: Needle diameter (gauge)	L: Distance of Drop (cm)	% yield	% EE
700	0.5	1	1	3000	1	300	200.01	50	26	20	71.38± 0.21	71.33 ± 0.51
500	0.75	3	3	2000	2	200	142.395	125	24	15	70.86 ± 0.65	63.54 ± 0.47
300	0.5	5	1	3000	3	100	200.01	200	26	10	50.44 ± 0.93	41.00 ± 0.05
700	1	1	5	3000	3	100	84.78	50	26	10	77.81 ± 0.57	75.43 ± 0.26
700	0.5	5	5	1000	3	300	200.01	50	22	10	69.58 ± 0.18	67.70 ± 0.92
500	0.75	3	3	2000	2	200	142.395	125	24	15	70.09 ± 0.42	64.01 ± 0.71
300	0.5	1	1	1000	1	100	84.78	50	22	10	49.98 ± 0.03	38.96 ± 0.09
700	1	1	1	1000	3	100	200.01	200	22	20	73.22 ± 0.69	70.21 ± 1.52
300	1	5	1	3000	3	300	84.78	50	22	20	56.33 ± 0.84	41.66 ± 0.60
700	0.5	5	5	3000	1	100	84.78	200	22	20	73.8 ± 0.79	68.47 ± 0.46
300	0.5	1	5	1000	3	300	84.78	200	26	20	49.06 ± 0.04	35.80 ± 0.15
300	1	1	5	3000	1	300	200.01	200	22	10	56.26 ± 0.10	42.60 ± 0.03
300	1	5	5	1000	1	100	200.01	50	26	20	52.76 ± 0.48	44.10 ± 0.96
500	0.75	3	3	2000	2	200	142.395	125	24	15	71.87 ± 0.29	64.00 ± 0.89
700	1	5	1	1000	1	300	84.78	200	26	10	72.9 ± 0.61	70.74 ± 0.24

Table 3 Box–Behnken design matrix and observed responses for optimization of quetiapine fumarate-loaded lipid nanoconjugates (QF-LNCs).

[1]Low (−1), center (0), and high (+1) levels represent the actual values used in the experimental design. PVA = Polyvinyl alcohol; DCM = Dichloromethane.

A: Lipid Conc (mg)	B: PVA Conc (%w/v)	C:Stirring speed (rpm)	%Yield	% EE	Particle Size (nm)
700	0.5	2000	68.51 ± 1.02	43.07 ± 1.54	606.42 ± 1.29
500	0.5	1000	78.4 ± 1.63	59.03 ± 1.23	449.23 ± 1.61
300	0.5	2000	54.45 ± 1.75	51.4 ± 1.44	485.73 ± 1.75
500	0.75	2000	83.64 ± 1.39	63.55± 1.71	329.3 ± 0.11
500	1	1000	81.43 ± 0.85	61.89 ± 0.81	415.37 ± 0.43
300	0.75	1000	52.93 ± 0.41	53.29 ± 1.92	462.68 ± 1.88
500	1	3000	84.12± 1.78	61.48 ± 1.30	428.41 ± 1.38
700	0.75	1000	67.83 ± 1.12	45.25 ± 1.58	584.33 ± 1.81
300	1	2000	57.31 ± 1.37	51.43 ± 1.20	482.94 ± 1.47
700	0.75	3000	68.09 ± 1.94	46.72 ± 1.62	548.81 ± 1.35
500	0.75	2000	82.89 ± 0.27	62.7 ± 1.93	401.01 ± 1.16
500	0.75	2000	83.11 ± 0.51	63.19 ± 1.99	371.27 ± 1.73
700	1	2000	69 ± 1.87	47.67 ± 1.37	520.69 ± 1.28
500	0.5	3000	80.39 ± 1.22	57.78 ± 1.47	457.09 ± 1.50
300	0.75	3000	55.22 ± 1.91	50.83 ± 1.73	490.55 ± 1.92

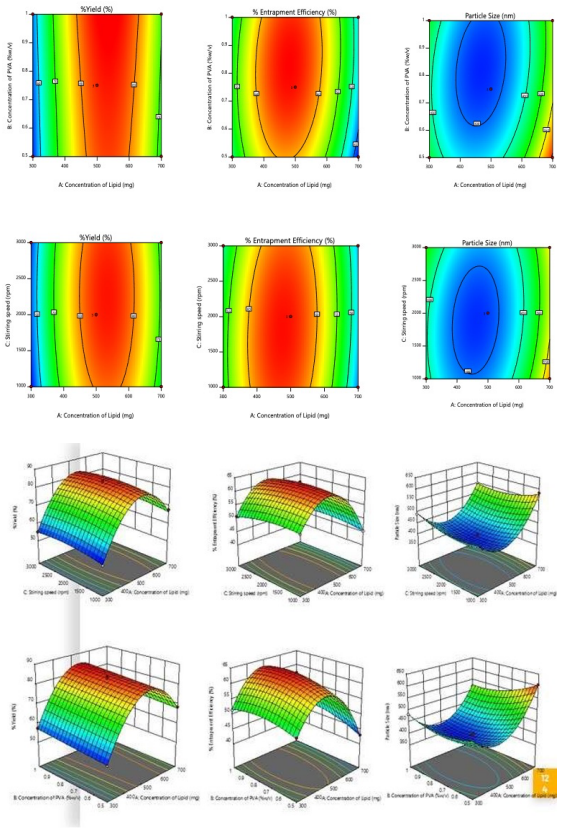

between the formulation variables and their influence on the optimization responses generated using the Box–Behnken design.

The three critical variables identified through the Plackett–Burman screening study, namely lipid concentration (X_1), PVA concentration (X_2), and stirring speed (X_4), were subsequently investigated in detail using a Box–Behnken design to optimize the formulation responses. The selected responses were percentage yield (Y_1), entrapment efficiency (Y_2), and particle size (Y_3). A total of 15 experimental runs were generated, and the corresponding experimental responses are presented in Table 3. The percentage yield, entrapment efficiency, and particle size varied considerably across the experimental design space, with percentage yield ranging from 52.93 to 84.12%, entrapment efficiency from 43.07 to 63.55%, and particle size from 329.30 to 606.42 nm. These variations demonstrated the sensitivity of QF-LNC characteristics to changes in lipid concentration, PVA concentration, and stirring speed. The experimental data were subjected to regression analysis using polynomial models to establish quantitative relationships between the independent variables and the measured responses. The statistical significance of the models and individual terms was evaluated by analysis of variance (ANOVA). The resulting response surface methodology models provided a systematic assessment of the influence of lipid concentration, PVA concentration, and stirring speed on the performance of QF-LNCs. The high coefficient of determination values obtained for the fitted models, together with close agreement between adjusted and predicted R^2 values, indicated satisfactory model fitting and predictive capability within the investigated design space. The significant model terms were subsequently used to interpret the individual, interaction, and curvature effects of the formulation variables.

The response behavior demonstrated that the three responses did not respond identically to the formulation variables. Percentage yield showed a pronounced nonlinear dependence on lipid concentration, with the response increasing substantially as lipid concentration was increased from the lower level toward the central region and subsequently showing a tendency toward a plateau or decline at the highest level. This behavior indicates that an optimum lipid concentration exists within the investigated range rather than a simple continuously increasing relationship. Entrapment efficiency was also influenced strongly by lipid and PVA concentrations, with the highest values observed around the intermediate lipid concentration and moderate-to-high PVA levels. Particle size exhibited a more complex response, with the lowest particle size observed at an intermediate lipid concentration and PVA concentration, demonstrating that excessive lipid concentration did not necessarily produce smaller particles.

The quadratic behavior observed for percentage yield indicated that the response was influenced not only by the direct effects of lipid concentration, PVA concentration, and stirring speed but also by curvature within the experimental design space. Lipid concentration exhibited the most pronounced positive linear influence on percentage yield, whereas PVA concentration and stirring speed contributed comparatively smaller positive effects. The negative quadratic effect associated predominantly with lipid concentration

demonstrated that the response did not increase indefinitely with increasing lipid concentration. Instead, the yield increased up to an optimum region and subsequently showed a reduction at the highest lipid level.

The positive effect of lipid concentration on yield can be attributed to the greater availability of the lipid matrix for formation and recovery of QF-LNCs. Increasing the amount of stearic acid provides a larger matrix in which the drug can be incorporated and facilitates formation of a more substantial lipid phase during solvent evaporation. However, excessive lipid concentration can increase the viscosity of the organic phase and may adversely affect dispersion and solvent diffusion, thereby explaining the observed curvature in the response. The PVA concentration also showed a positive contribution to yield, which can be attributed to improved stabilization of the dispersed lipid droplets and reduced coalescence during formation of the nanoconjugates. Stirring speed contributed positively to yield within the investigated range, presumably because enhanced mixing promotes dispersion of the organic phase and facilitates solvent removal and lipid solidification.

The coded polynomial relationship for Y_1 should be presented using the reduced model generated by Design-Expert. Based on the experimental data, the reduced relationship can be represented in the general form:

$$Y_1 = 82.958 + 6.690X_1 + 1.264X_2 + 0.904X_4 - 20.450X_1^2 - 1.682X_4^2$$

where X_1, X_2, and X_4 represent the coded levels of lipid concentration, PVA concentration, and stirring speed, respectively. The positive linear coefficients indicate that increasing the respective factors within the investigated region tends to increase percentage yield, whereas the negative quadratic coefficients demonstrate the presence of curvature and an optimum region, particularly for lipid concentration. The response surface analysis indicated that lipid concentration was an important determinant of QF encapsulation. The negative linear coefficient associated with lipid concentration, together with its significant quadratic contribution, indicates that increasing lipid concentration beyond the optimum region did not further improve entrapment efficiency. At an appropriate lipid level, the greater availability of the hydrophobic lipid matrix facilitates incorporation of quetiapine fumarate and reduces drug diffusion into the external aqueous phase during emulsification and solvent evaporation. However, excessive lipid concentration may alter the viscosity and dispersion characteristics of the organic phase, resulting in less efficient drug incorporation.

PVA concentration exerted a positive linear influence on entrapment efficiency and also contributed significant curvature effects. Increasing PVA concentration can improve stabilization of the dispersed lipid droplets and reduce coalescence during formulation, thereby favoring retention of drug within the lipid matrix. The interaction between lipid concentration and PVA concentration further indicates that the effect of one formulation component was dependent on the level of the other. Similarly, the interaction between lipid concentration and stirring speed suggests that the efficiency of drug incorporation was influenced by the combined effect of lipid content and mixing intensity rather than by either factor independently.

The reduced coded equation for Y_2 can be expressed as:

$$Y_2 = 63.147 - 3.030X_1 + 1.399X_2 + 1.143X_1X_2 + 0.983X_1X_4 - 12.888X_1^2 - 1.866X_2^2 - 1.236X_4^2$$

The negative coefficient of X_1 indicates that excessive lipid concentration reduced entrapment efficiency within the investigated region, whereas the positive coefficient for X_2 demonstrates the favorable contribution of PVA concentration. The significant interaction terms further confirm that the effect of lipid concentration on entrapment efficiency was dependent on PVA concentration and stirring speed. The significant quadratic terms demonstrate that an intermediate optimum exists for the formulation variables rather than a simple linear relationship.

Lipid concentration exerted the most important direct effect on particle size. Increasing lipid concentration beyond the optimum level resulted in larger particles, which may be associated with increased viscosity of the dispersed phase and reduced efficiency of droplet disruption during emulsification. The quadratic effect of lipid concentration further demonstrates that particle size did not change linearly across the investigated range. PVA concentration also showed a nonlinear influence on particle size. At an appropriate concentration, PVA can efficiently stabilize newly formed droplets, prevent their coalescence, and facilitate formation of smaller particles. However, excessive stabilizer concentration may increase the viscosity of the external phase and alter the interfacial characteristics of the system, thereby limiting further particle-size reduction.

Stirring speed showed a comparatively smaller direct effect than lipid concentration, but its contribution to the response cannot be disregarded. Increased agitation promotes dispersion of the organic phase and enhances solvent diffusion; however, the effect depends on the composition and viscosity of the formulation. Thus, the particle-size response reflects the combined influence of formulation composition and processing conditions.

The reduced coded equation for Y_3 can be expressed as:

$$Y_3 = 367.193 + 42.294X_1 + 120.410X_1^2 + 36.342X_2^2 + 33.990X_4^2$$

The positive coefficient for X_1 and its positive quadratic term indicate that increasing lipid concentration, particularly toward the higher end of the investigated range, favored an increase in particle size. The significant quadratic terms for lipid concentration, PVA concentration, and stirring speed demonstrate that particle size was governed predominantly by curvature effects rather than by simple linear changes across the design space.

The statistical findings were further supported by two-dimensional contour plots and three-dimensional response surface plots generated from the Box–Behnken design. These graphical representations provided a visual assessment of the influence of lipid concentration, PVA concentration, and stirring speed on percentage yield, entrapment efficiency, and particle size. The contour plots presented in Figure 3 demonstrate the distribution of the responses across the experimental design space, while the corresponding three-dimensional response surface plots in Figure 4 illustrate the changes in each response as the formulation variables were simultaneously varied.

For percentage yield, the response surface demonstrated a marked increase as lipid concentration increased from the lower level toward the intermediate region. The response subsequently approached a maximum region, followed by a reduction at higher lipid concentrations. This curved response is consistent with the significant quadratic contribution of lipid concentration and indicates that an intermediate-to-high lipid concentration is favorable for maximizing recovery of QF-LNCs. PVA concentration produced a positive contribution to yield, whereas stirring speed produced a comparatively smaller effect. The non-linear nature of the response surface indicates that simply increasing all three variables simultaneously would not necessarily provide the maximum yield.

For entrapment efficiency, the contour and response surface plots showed that the highest response occurred around the central lipid concentration and intermediate PVA concentration. The maximum experimentally observed entrapment efficiency was 63.55 ± 1.71% at 500 mg lipid, 0.75% PVA, and 2000 rpm. The curved response surface further indicates that excessive lipid concentration did not improve drug entrapment and that an optimum combination of lipid and PVA concentrations was required. The interaction between lipid concentration and PVA concentration was particularly relevant because stabilization of the dispersed lipid droplets must be balanced against the amount of lipid available for drug incorporation.

The particle-size response surface showed a distinct minimum region around the intermediate lipid and PVA concentrations. The lowest experimentally observed particle size was 329.30 ± 0.11 nm at 500 mg lipid, 0.75% PVA, and 2000 rpm. Increasing lipid concentration toward 700 mg resulted in considerably larger particles, reaching 606.42 ± 1.29 nm at 700 mg lipid, 0.5% PVA, and 2000 rpm. These findings indicate that excessive lipid loading may increase the viscosity of the organic phase and promote formation of larger droplets, whereas an appropriate PVA concentration favors stabilization and limits particle growth.

The combined response surface analysis therefore demonstrated that the optimum region was not defined by the maximum or minimum level of a single variable. Instead, the desired QF-LNC characteristics resulted from an appropriate balance among lipid concentration, PVA concentration, and stirring speed. The overlay plot shown in Figure 5 identified the region of the experimental design space in which the predefined criteria for percentage yield, entrapment efficiency, and particle size could be satisfied simultaneously.

To obtain a formulation providing a suitable overall balance among the three responses, a desirability function approach was employed. The optimization criteria were to maximize percentage yield (Y_1) and entrapment efficiency (Y_2), while minimizing particle size (Y_3). The desirability function integrates the individual desirability values of the responses and identifies the formulation region that provides the most appropriate simultaneous response. A desirability value approaching unity represents a highly desirable compromise among the selected response criteria.

To further evaluate the predictive capability and robustness of the developed BBD models, three checkpoint formulations were selected from different regions of the experimental design space. The checkpoint batches were deliberately selected using different combinations of lipid concentration, PVA concentration, and stirring speed to verify whether the developed models could reliably predict the responses beyond the central optimum region. The predicted and experimentally observed responses were subsequently compared, and percentage bias was calculated for each response.

The close agreement between predicted and experimentally observed values, particularly for entrapment efficiency and particle size, supports the predictive capability of the developed response surface models. However, the first checkpoint formulation for percentage yield showed a bias of approximately −6.05%, which is slightly greater than the commonly applied ±5% criterion. Therefore, it would be preferable not to state that all checkpoint biases were below 5%. Instead, the validation should be described as demonstrating generally good agreement, with most prediction errors below 5% and a slightly higher deviation observed for percentage yield in the first checkpoint formulation. This wording is more statistically defensible and directly reflects the values reported in Table 4.

Response	Result category	Selected batch for check point analysis		
		Batch 1	Batch 2	Batch 3
		X_1 = 750.00	X_1 = 750.00	X_1 =750.00
		X_2 = 1.00	X_2 = 0.750	X_2 = 0.750
		X_3= 125.00	X_3= 200.00	X_3= 50.00
Y_1 = %Yield	Predicted value	77.022	78.947	76.042
	Experimental value	72.631	75.290	74.086
	% Bias	-6.045	-4.857	-2.640
Y_2 = %EE	Predicted value	66.832	66.039	63.572
	Experimental value	65.736	64.907	63.509
	% Bias	-0.016	-1.744	-0.099
Y_3 = PS	Predicted value	323.008	314.008	393.258

Figure 3 Overlay plots generated using the desirability function approach showing the optimized formulation region for quetiapine fumarate-loaded lipid nanoconjugates (QF-LNCs). The highlighted region represents the combinations of formulation variables satisfying the desired criteria of maximum percentage yield and encapsulation efficiency with minimum particle size. Table 4 Comparison of predicted and experimental values obtained during checkpoint analysis for validation of the optimized Box–Behnken design model. The close agreement between predicted and observed responses confirms the reliability and predictive capability of the optimization model.

3.2 Particle Size, Zeta Potential, and Polydispersity Index (PDI)

The particle size of the optimized formulation was observed to be in the nanometric range, with a Z-average diameter of 400.5 nm as determined by dynamic light scattering analysis. The particle size obtained in the present study is comparable to that reported for lipid-based nanoparticulate systems prepared by solvent evaporation methods, which commonly exhibit particle sizes ranging from 200 to 500 nm. Previous studies on quetiapine-loaded lipid nanocarriers have similarly reported particle sizes within the nanometric range, demonstrating the suitability of lipid matrices for encapsulation and controlled drug delivery. The particle size obtained in the present study therefore falls within the acceptable range reported for quetiapine lipid nanocarrier systems.

The nanometric size of the formulation is an important factor contributing to enhanced dissolution and absorption characteristics, as smaller particles provide a larger specific surface area for interaction with the dissolution medium. The polydispersity index (PDI) value was found to be 0.5416, indicating a moderately broad particle size distribution. Although the PDI value is higher than that generally observed for highly monodisperse systems, it remains acceptable for lipid nanoconjugate formulations prepared by emulsification-solvent evaporation techniques. The observed distribution may be attributed to variations in droplet formation and lipid solidification during solvent evaporation. The particle size distribution profile demonstrated that the majority of particles were concentrated around the principal population with a mean intensity diameter of 386.3 nm, indicating successful formation of lipid nanoconjugates within the nanoscale range. The optimized formulation exhibited a particle size distribution characteristic of lipid-based particulate systems, as shown in Figure 6.

Zeta potential measurements were performed using a Malvern Panalytical ZS Xplorer at 25°C. The zeta potential value of the optimized QF-LNCs was found to be −21.88 mV with a conductivity of 8.705 mS/cm, indicating satisfactory colloidal stability. The negative surface charge suggests the presence of sufficient electrostatic repulsion among the particles, which minimizes aggregation and contributes to the stability of the nanosuspension. Similar negative zeta potential values have been reported for stearic acid-based lipid nanocarriers and are generally associated with acceptable dispersion stability.

The negative surface charge observed in the present lipid nanoconjugates can be primarily attributed to the ionization of residual carboxylic acid groups present on the surface of stearic acid molecules. In addition, adsorption of hydroxyl ions from the aqueous medium and the orientation of stabilizer molecules at the particle interface may further contribute to the measured surface charge. The magnitude of the zeta potential indicates that the formulation possesses sufficient electrostatic stabilization to reduce particle aggregation and maintain colloidal integrity during storage and handling. As evidenced in Figure 7, the zeta potential profile demonstrates that the lipid nanoconjugates possess adequate surface charge for maintaining satisfactory colloidal stability.

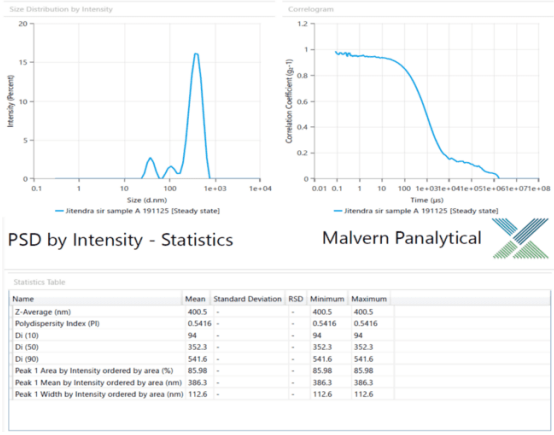

Figure 4Particle size distribution of optimized QF-LNCs determined by dynamic light scattering (DLS) using a Malvern Panalytical ZS Xplorer. Measurement conditions: 25°C, dispersion in distilled water. Z-average diameter = 400.5 nm, PDI = 0.5416. Data represent the mean of the measurement.

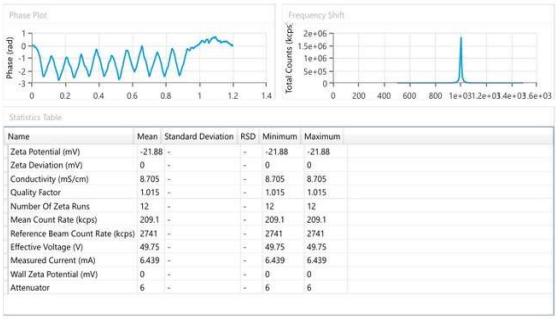

Name	Mean	Standard Deviation	RSD	Minimum	Maximum
Zeta Potential (mV)	-21.88	-	-	-21.88	-21.88
Zeta Deviation (mV)	0	-	-	0	0
Conductivity (mS/cm)	8.705	-	-	8.705	8.705
Quality Factor	1.015	-	-	1.015	1.015
Number Of Zeta Runs	12	-	-	12	12
Mean Count Rate (kcps)	209.1	-	-	209.1	209.1
Reference Beam Count Rate (kcps)	2741	-	-	2741	2741
Effective Voltage (V)	49.75	-	-	49.75	49.75
Measured Current (mA)	6.439	-	-	6.439	6.439
Wall Zeta Potential (mV)	0	-	-	0	0
Attenuator	6	-	-	6	6

Figure 5 Zeta potential distribution of optimized QF-LNCs measured by electrophoretic light scattering. Conditions: 25°C. Mean zeta potential = −21.88 mV, conductivity = 8.705 mS/cm. The negative surface charge indicates satisfactory colloidal stability of the lipid nanoconjugates.

3.2. Encapsulation Efficiency (% EE) and Drug Loading (DL)

Encapsulation Efficiency and Drug Loading

The encapsulation efficiency (EE) of the developed QF-LNCs was found to be in the range of 43.07 ± 1.54 to 63.55 ± 1.71%, which is comparable to previously reported quetiapine lipid-based nanoparticulate systems. Yasir et al. reported an entrapment efficiency of 75.92% for optimized quetiapine solid lipid nanoparticles. These findings indicate effective incorporation of quetiapine within the lipid carrier system(Yasir, Gaur, Puri, Shekhar, & Kumar, 2018). The encapsulation efficiency observed in the present study is consistent with previously reported lipid nanoparticle formulations, where hydrophobic drug-lipid interactions contributed to efficient drug entrapment.

The high EE is primarily due to the hydrophobic compatibility between the drug and the lipid, minimizing drug loss into the aqueous phase during the emulsification step. Additionally, the viscosity of the organic phase, governed by lipid concentration, plays a pivotal role in retaining the drug within the lipid droplets during solvent diffusion and nanoparticle solidification. The lipid matrix formed by stearic acid provides a hydrophobic environment that favors the incorporation of quetiapine fumarate and restricts its diffusion into the external aqueous phase during formulation, thereby contributing to enhanced entrapment efficiency.

% Drug content was determined for the optimized batch of QF-LNCs using a UV-visible spectrophotometric method at λmax of 209 nm. It was found to be 4.0 ± 0.28% w/w. Determination of drug content is essential for performing the in vitro drug release study, as the equivalent amount of drug present in the formulation can be accurately calculated from the percentage drug content. The observed drug content further confirms successful incorporation of quetiapine fumarate within the lipid nanoconjugates and indicates uniform distribution of the drug throughout the lipid matrix.

3.3. Shape and Surface Morphology (SEM)

The SEM micrograph showed predominantly spherical lipid nanoconjugates with well-defined boundaries and relatively smooth surfaces. Most of the particles were observed within the nanometric range, which is consistent with the particle size data obtained from dynamic light scattering analysis. The nanoconjugates appeared uniformly distributed throughout the field, indicating successful formation of the lipid-based carrier system. A limited degree of particle clustering was observed in certain regions, which may be attributed to aggregation occurring during sample preparation and drying prior to SEM analysis.

No prominent crystalline drug particles or irregular structures were visible on the particle surfaces, suggesting efficient incorporation of quetiapine fumarate within the lipid matrix. The absence of visible drug crystals further indicates that the drug was successfully entrapped within the nanoconjugates rather than remaining as free crystalline material on the particle surface. The spherical morphology obtained may be attributed to the solidification of stearic acid during solvent evaporation, resulting in the formation of discrete lipid nanoconjugates with smooth and compact surfaces.

The smooth surface morphology and relatively uniform particle distribution indicate the formation of stable lipid nanoconjugates and support the effectiveness of the solvent evaporation method employed for formulation development. The surface morphology of the optimized QF-LNCs is presented in Figure 8.

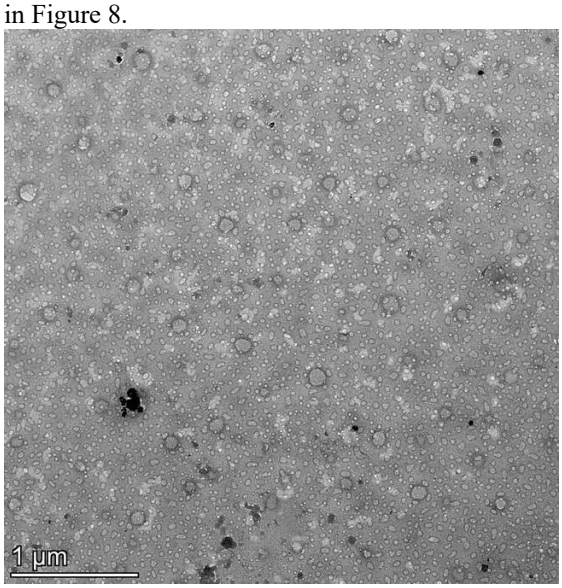

Figure 6 Scanning electron micrograph of optimized QF-LNCs. Sample was sputter-coated with gold prior to imaging. Scale bar = 1 µm. The micrograph reveals predominantly spherical lipid nanoconjugates with smooth surfaces and relatively uniform particle distribution. Limited aggregation is observed, which may be attributed to particle drying during sample preparation.

3.4. X-Ray Diffraction (XRD) Analysis

XRD analysis was performed to investigate the physical state of drug within the lipid nanoconjugates and to evaluate the effect of the formulation process on the crystallinity of the drug. The XRD diffractograms of pure quetiapine fumarate, stearic acid, and optimized QF-LNCs are presented in Figure 9.

The diffraction pattern of pure Quetiapine fumarate exhibited several sharp, intense, and well-defined peaks at distinct 2θ positions throughout the scanning range, confirming the highly crystalline nature of the drug. The presence of these characteristic diffraction peaks indicates the existence of a well-ordered crystal lattice structure in the pure drug. Similarly, stearic acid displayed intense and sharp diffraction peaks characteristic of a crystalline lipid material. The prominent peaks observed in the stearic acid diffractogram confirm its ordered molecular arrangement and high degree of crystallinity.

In contrast, the diffractogram of the optimized QF-LNCs exhibited a marked reduction in the intensity of the characteristic crystalline peaks of Quetiapine fumarate. Several prominent drug peaks were either significantly diminished, broadened, or completely absent in the optimized formulation. Furthermore, the diffraction pattern of the nanoconjugates showed a considerable decrease in overall crystallinity when compared with the pure drug and pure lipid. The reduction in peak intensity and broadening of diffraction signals suggest a substantial decrease in the ordered crystalline arrangement of quetiapine fumarate following formulation into lipid nanoconjugates.

The disappearance or weakening of the characteristic drug peaks may be attributed to the molecular dispersion of quetiapine fumarate within the stearic acid matrix and the formation of a less ordered solid-state structure. During solvent evaporation and lipid solidification, the drug molecules become entrapped within the lipid matrix, restricting crystal growth and preventing recrystallization of the drug into its original crystalline form. Such behavior is commonly observed in lipid-based nanocarrier systems, where the encapsulated drug exists in an amorphous or partially amorphous state within the lipid core.

The observed reduction in crystallinity is considered advantageous for drug delivery applications because amorphous materials generally possess higher free energy and greater molecular mobility than their crystalline counterparts. Consequently, the partial conversion of Quetiapine fumarate from a crystalline to an amorphous or molecularly dispersed state is expected to enhance drug wettability, apparent solubility, and dissolution rate. The XRD findings therefore provide strong evidence for the successful incorporation of Quetiapine fumarate into the lipid matrix and support the formation of stable lipid nanoconjugates with altered solid-state characteristics.

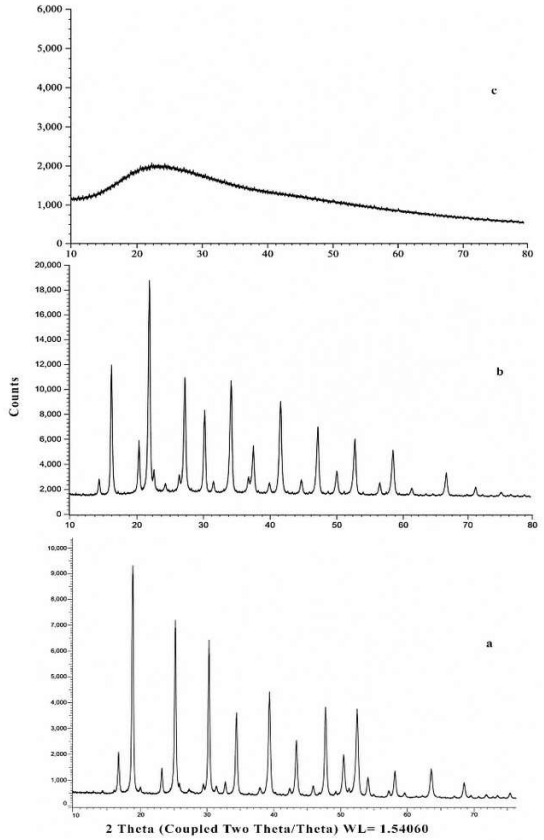

Figure 7 X-ray diffraction patterns of (a) pure Quetiapine fumarate, (b) stearic acid, and (c) optimized QF-LNCs. Pure Quetiapine fumarate and stearic acid exhibited characteristic sharp crystalline peaks, whereas the optimized QF-LNCs showed reduced peak intensity and partial disappearance of characteristic drug peaks, indicating reduced crystallinity and molecular dispersion of Quetiapine fumarate within the lipid matrix.

3.5 Fourier transform infrared spectroscopy (FT-IR)

To assess the compatibility of quetiapine fumarate with stearic acid and to identify any possible chemical interactions during formulation development, Fourier transform infrared (FTIR) spectroscopy was performed. Retention of the characteristic functional group peaks in the FTIR spectra presented in Figure 10 further confirmed the compatibility of the drug with the lipid matrix. The FTIR spectrum of pure quetiapine fumarate (a) showed characteristic absorption bands at approximately 3443 cm^{-1}, corresponding to N–H stretching vibrations, and 1595–1575 cm^{-1}, which were assigned to aromatic C=C stretching vibrations. Additional peaks observed in the fingerprint region were associated with C–N stretching and heterocyclic ring vibrations characteristic of quetiapine fumarate. The FTIR spectrum of stearic acid (b) exhibited characteristic absorption bands around 2918 and 2850 cm^{-1}

corresponding to aliphatic C–H stretching vibrations, while the strong absorption band near 1700 cm^{-1} was attributed to the carbonyl (C=O) stretching vibration of the carboxylic acid group.

The physical mixture of quetiapine fumarate and stearic acid (c) showed the characteristic peaks of both the drug and lipid without any significant shift or disappearance, indicating the absence of chemical interaction when the components were simply mixed. In the optimized lipid nanocarrier formulation (d), the major characteristic peaks of quetiapine fumarate and stearic acid were retained, although slight peak broadening and minor variations in peak intensity were observed. These changes may be attributed to intermolecular interactions and physical incorporation of the drug within the lipid matrix. Importantly, no new peaks appeared and no significant shifts in the characteristic absorption bands were detected, indicating the absence of chemical incompatibility or drug degradation during the formulation process.

The preservation of the characteristic functional group peaks in the optimized QF-LNC formulation suggests that quetiapine fumarate remained chemically stable and was successfully incorporated into the stearic acid matrix predominantly through physical entrapment rather than chemical interaction.

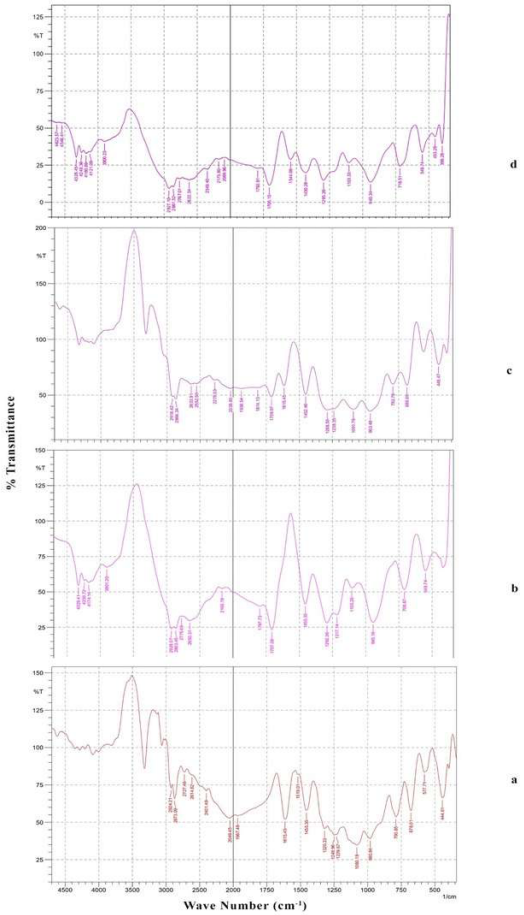

Figure 8 Fourier transform infrared (FTIR) spectra of (a) pure quetiapine fumarate (QF), (b) pure stearic acid (SA), (c) physical mixture (QF+SA), and (d) optimized QF-LNCs. Key absorption bands (cm^{-1}): QF – 3443 (N–H stretching), 1595–1575 (aromatic C=C stretching); SA – 2918 and 2850 (aliphatic C–H stretching), ~1700 (C=O stretching). No new peaks or significant shifts indicate drug–lipid compatibility and successful incorporation of quetiapine fumarate within the lipid nanocarrier matrix.

3.6 Differential scanning calorimetry (DSC)

Differential scanning calorimetry (DSC) was employed to investigate the thermal behavior of quetiapine fumarate and the optimized quetiapine fumarate-loaded lipid nanocarriers (QF-LNCs). The DSC thermograms of pure quetiapine fumarate and the optimized QF-LNC formulation are presented in Figure 11. The thermogram of pure quetiapine fumarate (a) exhibited a sharp and intense endothermic peak at approximately 180°C, corresponding to its characteristic melting point and confirming the crystalline nature of the drug. The presence of a well-defined melting endotherm indicates that quetiapine fumarate exists in a highly ordered crystalline state.

In contrast, the DSC thermogram of the optimized QF-LNCs (b) showed a marked reduction in the intensity of the characteristic drug melting peak along with peak broadening and a slight shift toward a lower temperature region (approximately 155–160°C). The absence or substantial reduction of the sharp melting endotherm of quetiapine fumarate suggests a decrease in drug crystallinity and indicates that the drug was successfully incorporated within the lipid matrix. This behavior may be attributed to the conversion of the drug from a crystalline state to an amorphous or molecularly dispersed form within the lipid nanocarrier system.

The observed thermal changes further support the encapsulation of quetiapine fumarate within the stearic acid matrix and indicate effective drug–lipid interaction at the physical level. Furthermore, no additional endothermic or exothermic peaks indicative of degradation products were observed, suggesting that the drug remained thermally stable during the formulation process.

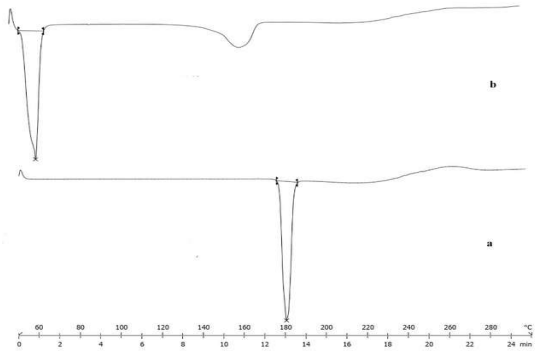

Figure 9 Differential scanning calorimetry thermograms of (a) pure quetiapine fumarate and (b) optimized QF-LNCs. Pure QF exhibited a sharp

endothermic melting peak at approximately 180°C, confirming its crystalline nature. The optimized QF-LNCs showed a broadened and less intense endothermic peak at a lower temperature, indicating reduced crystallinity and successful incorporation of quetiapine fumarate within the lipid matrix.

3.7 In-Vitro drug release

The cumulative drug release reached 85.78 ± 2.49% at 24 h, with an initial release of approximately 18.50% during the first hour in acidic medium (pH 1.2) followed by a gradual and controlled release after transfer to phosphate buffer (pH 6.8). The release increased steadily from 29.79% at 2 h to 78.51% at 12 h, eventually reaching 85.78% at 24 h, indicating efficient drug encapsulation and prolonged release from the lipid nanocarrier matrix. The absence of abrupt fluctuations in the release profile suggests good formulation stability under varying pH conditions and effective retention of the drug within the lipidic core.

The optimized LNC formulation demonstrated a characteristic biphasic release pattern consisting of an initial burst release followed by a prolonged sustained-release phase. The initial release may be attributed to drug molecules adsorbed or weakly associated with the particle surface, whereas the subsequent controlled release is likely governed by diffusion of quetiapine fumarate through the lipid matrix and gradual erosion or reorganization of the carrier system. The release profile is presented in Figure 12.

The dissolution data were fitted to various kinetic models, and the corresponding regression coefficients (R^2) are summarized in Table 5. Among the investigated models, the first-order model (R^2 = 0.983) provided the best fit, indicating that the drug release rate was dependent on the remaining drug concentration within the nanocarriers. The Higuchi model (R^2 = 0.956) also showed a high degree of correlation, suggesting diffusion-controlled release from the lipid matrix. Furthermore, the relatively high Hixson–Crowell coefficient (R^2 = 0.930) implies that changes in particle surface area and geometry may contribute to the release mechanism during dissolution. In contrast, the zero-order model (R^2 = 0.845) exhibited comparatively lower correlation, indicating that the formulation does not release the drug at a constant rate throughout the dissolution period. Collectively, these findings suggest that drug release from the optimized LNC formulation is predominantly governed by concentration-dependent diffusion with a contribution from matrix structural changes.

The sustained-release performance of the optimized LNC formulation is advantageous for oral delivery of quetiapine fumarate, as it may reduce dosing frequency and maintain therapeutic drug concentrations for an extended duration. Similar sustained-release characteristics have been reported for quetiapine-loaded lipid-based nanocarriers, where diffusion through the lipid matrix was identified as the primary mechanism controlling drug release.

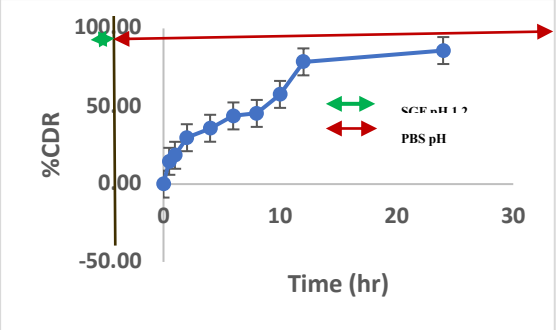

Figure 10 In vitro drug release profile of the optimized quetiapine fumarate-loaded lipid nanocarriers (QF-LNCs) in simulated gastric fluid (SGF, pH 1.2) for 2 h followed by simulated intestinal fluid (SIF, pH 6.8) up to 24 h (n = 3, mean ± SD). The formulation exhibited an initial burst release (~18.5% in 1 h) followed by sustained drug release, reaching 85.78 ± 2.49% at 24 h. Release kinetics were best described by first-order (R^2 = 0.983) and Higuchi (R^2 = 0.956) models.

Table 5. Regression coefficients (R^2 values) for different kinetic models of the optimized QF-LNC formulation.

Model	**R^2**
Zero order	0.845
First order	0.983
Higuchi	0.956
Hixson-Crowell	0.93

3.8 Stability Studies

The stability of the optimized QF-LNCs formulation was evaluated under different storage conditions according to ICH guidelines, and the results are presented in Table 6. The stability study was conducted to assess the effect of storage temperature and humidity on the physicochemical characteristics of the formulation over a period of six months. Parameters including particle size, PDI, zeta potential, and % EEwere monitored at predetermined intervals. The stability assessment was primarily intended to evaluate trends in formulation properties during storage. Although formal statistical analysis of the stability data was not performed, the observed changes remained minimal and within acceptable limits throughout the study period.

Samples stored at 4 ± 2 °C were maintained in closed containers under refrigerated conditions, whereas long-term and accelerated stability studies were carried out at 25 ± 2 °C/60 ± 5% RH and 40 ± 2 °C/75 ± 5% RH, respectively. The optimized QF-LNC formulation exhibited good physical stability under all storage conditions during the six-month study period.

Under refrigerated storage conditions (4 ± 2 °C), only slight changes were observed in the measured parameters. The particle size increased marginally from 400.50 ± 1.73 nm to 402.03 ± 1.34 nm after six months. The PDI remained nearly constant, varying from 0.541 to 0.542, indicating maintenance of a relatively uniform particle size distribution. Similarly, the zeta potential showed negligible variation, changing from −21.88 ± 1.70 mV to −21.93 ± 2.60 mV. A slight decrease in entrapment efficiency from 63.55 ± 1.71% to 62.12 ± 1.45% was observed, suggesting minimal drug leakage from the lipid matrix during storage.

At 25 ± 2 °C/60 ± 5% RH, the formulation retained its physicochemical characteristics with only minor variations. The particle size increased slightly to 402.61 ± 1.86 nm after six months, while the PDI remained within a narrow range of 0.541–0.544. The zeta potential remained relatively stable throughout the study period, indicating preservation of colloidal stability. Entrapment efficiency gradually decreased to 60.97 ± 1.34%, indicating limited drug loss during storage under room-temperature conditions.

Under accelerated conditions (40 ± 2 °C/75 ± 5% RH), comparatively greater changes were observed in the physicochemical properties of the formulation. The particle size increased to 405.91 ± 1.60 nm after six months, accompanied by a slight increase in PDI from 0.541 to 0.547. Although the zeta potential remained relatively unchanged, a more pronounced decline in entrapment efficiency was observed, decreasing from 63.55 ± 1.71% to 59.36 ± 1.54%. The reduction in entrapment efficiency may be attributed to increased molecular mobility within the lipid matrix and partial diffusion of the entrapped drug under elevated temperature and humidity conditions. However, no visible signs of aggregation, precipitation, or phase separation were observed throughout the study period.

Overall, the optimized QF-LNC formulation demonstrated good physical stability under all tested storage conditions. However, the variations in particle size, PDI, zeta potential, and entrapment efficiency were comparatively lower under refrigerated (4 ± 2 °C) and room-temperature (25 ± 2 °C/60 ± 5% RH) conditions than under accelerated storage conditions. The particle size remained close to the initial value, the surface charge was largely preserved, and only a slight reduction in entrapment efficiency was observed. Therefore, the formulation can be considered stable under refrigerated and room-temperature storage conditions, indicating its suitability for long-term storage and pharmaceutical application.

Table 6. *Stability study data of the optimized quetiapine fumarate-loaded lipid nanocarrier (QF-LNC) formulation under different storage conditions for six months.*

Temp (°C)/ RH (%)	**Time (Months)**	**Particle Size (nm)**	**PDI**	**Zeta Potential (mV)**	**Entrapment Efficiency (%)**
4±2 °C	0	400.50 ± 1.73	0.541	-21.88 ± 1.7	63.55± 1.71
	1	400.85 ± 1.54	0.541	-21.89 ± 1.5	63.14 ± 1.20
	3	401.14 ± 1.82	0.542	-21.91 ± 1.2	62.57 ± 1.94
	6	402.03 ± 1.34	0.542	-21.93 ± 2.6	62.12 ± 1.45
25±2 °C / 60±5 % RH	0	400.5 ± 1.73	0.541	-21.88 ± 1.7	63.55± 1.71
	1	401.4 ± 1.04	0.542	-21.90 ± 1.2	62.15 ± 1.24
	3	401.87 ± 1.57	0.542	-21.92 ± 1.3	61.78 ± 1.98
	6	402.61 ± 1.86	0.544	-21.94 ± 2.6	60.97 ± 1.34
40±2 °C / 75±5 % RH	0	400.5 ± 1.73	0.541	-21.88 ± 1.7	63.55± 1.71
	1	401.2 ± 1.02	0.543	-21.91 ± 1.9	61.39 ± 1.85
	3	403.35 ± 1.98	0.544	-21.92 ± 2.3	60.53 ± 1.27
	6	405.91 ± 1.60	0.547	-21.96 ± 3.9	59.36 ± 1.54

Conclusion

In the present investigation, a statistically guided experimental design approach was successfully employed for the development and optimization of quetiapine fumarate-loaded lipid nanoconjugates (QF-LNCs) using the solvent evaporation technique. The Plackett–Burman design efficiently identified the critical formulation and process variables affecting percentage yield and encapsulation efficiency, while the Box–Behnken design enabled systematic optimization of lipid concentration, PVA concentration, and stirring speed to obtain an optimized formulation with desirable physicochemical characteristics. The optimized QF-

LNCs exhibited nanoscale particle size, satisfactory surface charge, acceptable encapsulation efficiency, and uniform morphology, demonstrating the robustness and reproducibility of the formulation strategy.

Comprehensive characterization studies, including SEM, FTIR, DSC, and XRD analyses, confirmed successful incorporation of quetiapine fumarate within the lipid matrix without evidence of chemical incompatibility. The optimized formulation exhibited a biphasic drug release profile characterized by an initial burst release followed by sustained drug release over 24 h, with release kinetics predominantly governed by first-order diffusion and matrix-controlled mechanisms. Furthermore, the formulation maintained its physicochemical properties under refrigerated and long-term storage conditions, indicating satisfactory stability and suitability for pharmaceutical applications.

Overall, the developed lipid nanoconjugate system represents a promising oral drug delivery approach for improving the dissolution behavior and sustained release of quetiapine fumarate. The optimized formulation has the potential to enhance therapeutic performance, reduce dosing frequency, and improve patient compliance. Nevertheless, further in vivo pharmacokinetic, pharmacodynamic, and long-term safety studies are required to establish its bioavailability, therapeutic efficacy, and clinical applicability.

Author contributions

Chitrali Talele contributed to the conceptualization of the manuscript, writing of the original draft, critical review, and overall manuscript development. Payal Vaja and Chetan Borkhataria was responsible for data refinement and provided final approval of the manuscript prior to submission.

Acknowledgments

The authors gratefully acknowledge the institutional support and academic environment provided by Dr. Subhash University, Junagadh, Gujarat, India, which facilitated the completion of this work.

AI disclosure statement

The authors used ChatGPT (OpenAI) solely for language editing and improvement of sentence clarity during manuscript revision. The authors reviewed and edited all generated content and take full responsibility for the final manuscript. No AI tools were used for data analysis, interpretation of results, or generation of figures.

Conflict of interest

The authors declare that there are no conflicts of interest related to this work.

Data availability statement

The datasets generated and/or analyzed during the current study are available from the corresponding author on reasonable request.

Ethics Statement

Ethical approval was not required for this study, as the research involved only in vitro formulation development and characterization and did not involve human participants, animals, or human/animal-derived biological samples.

Financial support and sponsorship

This research did not receive any specific grant from funding agencies in the public, commercial, or not for profit sectors.

List of Abbreviations

ANOVA - Analysis of Variance
BBD- Box–Behnken Design
DCM-Dichloromethane
DL-Drug Loading
DLS-Dynamic Light Scattering
DSC-Differential Scanning Calorimetry
EE-Encapsulation Efficiency
FTIR-Fourier Transform Infrared Spectroscopy
ICH-International Council for Harmonisation
LNCs-Lipid Nanoconjugates
PBD-Plackett–Burman Design
PBS-Phosphate Buffered Saline
PDI-Polydispersity Index
PVA-Polyvinyl Alcohol
QF-Quetiapine Fumarate
QF-LNCs-Quetiapine Fumarate-Loaded Lipid Nanoconjugates
RH-Relative Humidity
SD-Standard Deviation
SEM-Scanning Electron Microscopy
SGF-Simulated Gastric Fluid
SIF-Simulated Intestinal Fluid
XRD-X-ray Diffraction

REFERENCES

Abdel-Bar, H. M., Tulbah, A. S., Darwish, H. W., Salama, R., Naguib, I. A., Yassin, H. A., & Abo El-Enin, H. A. (2023). Quetiapine Albumin Nanoparticles as an Efficacious Platform for Brain Deposition and Potentially Improved Antipsychotic Activity. *Pharmaceutics, 15*(7). doi:https://doi.org/10.3390/pharmaceutics15071785

Aboti, P., Shah, P., Patel, D., & Dalwadi, S. (2014). Quetiapine fumarate loaded solid lipid nanoparticles for improved oral bioavailability. *Drug Delivery Letters, 4*(2), 170-184. doi:https://doi.org/10.2174/2210303104021408051051 27

Behbahani, E. S., Ghaedi, M., Abbaspour, M., & Rostamizadeh, K. (2017). Optimization and characterization of ultrasound assisted preparation of curcumin-loaded solid lipid nanoparticles: Application of central composite design, thermal analysis and X-ray diffraction techniques. *Ultrasonics Sonochemistry, 38*, 271-280. doi:https://doi.org/10.1016/j.ultsonch.2017.03.013

Chauhan, R. (2026). Advancements in polymer- and lipid-based nanoparticles for enhancing drug solubility, stability, and bioavailability: an integrative and forward-looking review. *Frontiers in Nanotechnology, Volume 8 - 2026*. doi:https://doi.org/10.3389/fnano.2026.1801422

Ding, Y., Nielsen, K. A., Nielsen, B. P., Bøje, N. W., Müller, R. H., & Pyo, S. M. (2018). Lipid-drug-conjugate (LDC) solid lipid nanoparticles (SLN) for the delivery of nicotine to the oral cavity – Optimization of nicotine loading efficiency. *European Journal of Pharmaceutics and Biopharmaceutics, 128*, 10-17. doi:https://doi.org/10.1016/j.ejpb.2018.03.004

Duong, V. A., Nguyen, T. T., & Maeng, H. J. (2020). Preparation of Solid Lipid Nanoparticles and Nanostructured Lipid Carriers for Drug Delivery and the Effects of Preparation Parameters of Solvent Injection Method. *Molecules, 25*(20). doi:10.3390/molecules25204781

Kelidari, H. R., Saeedi, M., Akbari, J., Morteza-Semnani, K., Gill, P., Valizadeh, H., & Nokhodchi, A. (2015). Formulation optimization and in vitro skin penetration of spironolactone loaded solid lipid nanoparticles. *Colloids and Surfaces B: Biointerfaces, 128*, 473-479. doi:https://doi.org/10.1016/j.colsurfb.2015.02.046

Noorulla, K. M., Yasir, M., Muzaffar, F., Ghoneim, M. M., Almurshedi, A. S., Tura, A. J., . . . Ahmed, M. M. (2022). Intranasal delivery of chitosan decorated nanostructured lipid carriers of Buspirone for brain targeting: Formulation development, optimization and In-Vivo preclinical evaluation. *Journal of Drug Delivery Science and Technology, 67*, 102939. doi:https://doi.org/10.1016/j.jddst.2021.102939

Pooja, D., Tunki, L., Kulhari, H., Reddy, B. B., & Sistla, R. (2016). Optimization of solid lipid nanoparticles prepared by a single emulsification-solvent evaporation method. *Data in Brief, 6*, 15-19. doi:https://doi.org/10.1016/j.dib.2015.11.038

Riedel, M., Müller, N., Strassnig, M., Spellmann, I., Severus, E., & Möller, H. J. (2007). Quetiapine in the treatment of schizophrenia and related disorders. *Neuropsychiatr Dis Treat, 3*(2), 219-235. doi:https://doi.org/10.2147/nedt.2007.3.2.219

Shazly, G. A. (2017). Ciprofloxacin controlled-solid lipid nanoparticles: characterization, in vitro release, and antibacterial activity assessment. *BioMed research international, 2017*(1), 2120734. doi:https://doi.org/10.1155/2017/2120734

Yasir, M., Gaur, P. K., Puri, D., Shekhar, P., & Kumar, S. S. (2018). Solid lipid nanoparticles approach for lymphatic targeting through intraduodenal delivery of quetiapine fumarate. *Current drug delivery, 15*(6), 818-828. doi:https://doi.org/10.2174/1567201814666170525121049

Zielińska, A., Ferreira, N. R., Feliczak-Guzik, A., Nowak, I., & Souto, E. B. (2020). Loading, release profile and accelerated stability assessment of monoterpenes-loaded solid lipid nanoparticles (SLN). *Pharmaceutical Development and Technology, 25*(7), 832-844. doi:https://doi.org/10.1080/10837450.2020.1744008